Design of Asymmetric Slot Star Shape UWB Antenna for Wireless Applications

Tuhina Oli
M.Tech. Student
DIAT(Deemed University)
Girinagar, Pune – 411 025

Raj Kumar
Armament Electronics
ARDE, Pashan
Dr. Homi Baba Road, Pune - 21

Nagendra Kushwaha
RVS Ram krishna
Research Scholar
DIAT(DU),Girinagar,Pune-25

ABSTRACT
A new compact slot antenna is presented for UWB applications. The slot in the ground plane is asymmetric which helps in wide band impedance matching. The radiating element is a star shape geometry which is fed by a double stepped co-planar waveguide structure. Two antennas are designed with this geometry. Out of these two antennas one is proposed. The proposed antenna has an impedance bandwidth of 7.5 GHz (3.0-10.5 GHz). The radiation patterns are stable with respect to frequency and of bi-directional shaped in E-plane and Omni-directional shaped in H-plane. The measured and simulated results are in good agreement.

Keywords
Asymmetric slot antenna, CPW-fed antenna, UWB antenna and Star shape antenna.

1. INTRODUCTION
Federal Communication commission (FCC) in 2002 had issued guidelines for UWB implementation as well as data communication. According to FCC terminology, antenna bandwidth should be from 3.1 GHz to 10.6 GHz for unlicensed UWB applications. The ultra-wideband (UWB) radio system is getting increasingly popular for the academic and industrial applications. As the key component of the UWB wireless communication system, the UWB antenna [1-2] has drawn increasing attention. The feasible UWB antenna should be designed with compact size, good impedance matching, flat group delay and Omni-directional radiation patterns [3-10]. For the UWB applications, printed antennas have proved to be a good choice [4] as they are low profile, compact in size and can be easily integrated with monolithic microwave integrated circuits (MIC/MMICS). They may be incorporated with different slot geometries for further extension of bandwidth. Slots may be wide /narrow slots. Wider slots provide a greater improvement in bandwidth as compared to the narrow slots but have disadvantages of having larger size. On the other hand, the main limitation of narrow slots is their narrow bandwidth operation and because of it they cannot satisfy compactness and bandwidth requirement criteria needed for UWB application at same time [11-12]. Various slot geometries are reported that may maintain compactness in the size along with wider bandwidth for example " island like" space filling curves are quite popular for development of circularly polarized broadband antennas because of their space filling properties.
In this paper, a CPW-fed slot antenna for UWB application is presented. The slot in the ground plane is asymmetrically placed which provides improvement in the impedance matching for the antenna. The patch geometry is star shaped which is fed by a double stepped feed line. The antennas are simulated in CST Microwave studio. The reflection coefficient characteristic of the fabricated antenna is measured using Rohde & Schwarz Vector Network Analyzer (R&S ZVA-40) while the radiation patterns and gain are measured in the in-house anechoic chamber. Finally the simulated and measured results are compared.

2. ANTENNA GEOMETRY
Fig. 1 and Fig. 2 show the structural view of Antenna 1 and Antenna 2. The antennas are printed on one side of a FR4 Epoxy substrate of thickness h = 1.58 mm, relative permittivity ε_r = 4.3 and loss tangent tan δ = 0.0019. The patch is formed by inverting and adding two isosceles triangles having base width denoted T_b and height T_h which results into a star shaped structure (Fig. 2). The star shape patch is fed by a double stepped CPW feed which helps to achieve better impedance matching.

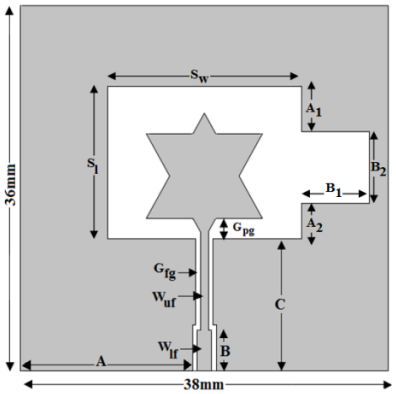

Fig 1: Geometry of Antenna 1

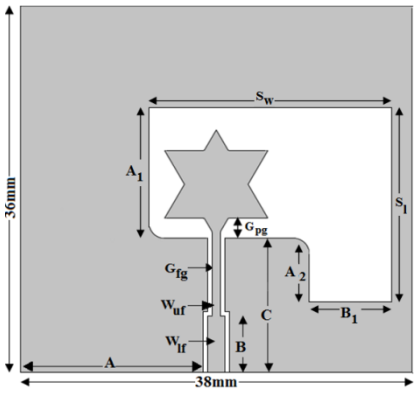

Fig 2: Geometry of Antenna 2

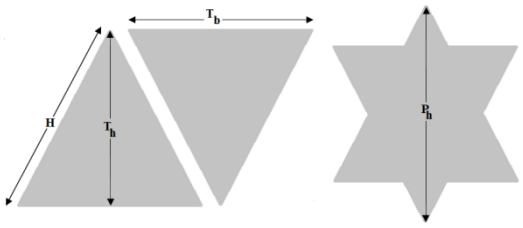

Fig 3: Front view of Patch scheme

Table 1. Various Parameters for Patch geometry

Parameters	Antenna 1 (in mm)	Antenna 2 (in mm)
T_b	12	10
T_h	10.39	8.66
H	12	10
P_h	12.39	10.66

For the slot, initially a simple symmetric rectangular shape is etched in the ground plane which provides a wide impedance bandwidth. Further to increase the bandwidth, the slot is made asymmetric by adding an additional rectangular slot on one side as seen from Fig. 1. Asymmetric nature of slot helps in achieving higher bandwidth as it provide an inductive behaviour which counters the capacitive effect of patch generated from fringing effect. Further enhancement in terms of bandwidth is done by changing the size of the slot. Also the slot shape is further modified as shown in Fig. 2. Finally, both the antennas have been designed with optimized dimensions as given in table 2.

Table 2. Optimized dimension (mm) of Antenna 1 and Antenna 2

Para-meters	Ant-1	Ant-2	Para-meters	Ant-1	Ant-2
G_{pg}	0.40	0.70	S_l	15	19.0
G_{fg}	0.30	0.40	S_w	20	23.5
W_{uf}	0.81	1.02	A_1	4.50	12.8
W_{lf}	1.50	1.93	A_2	3.50	6.50
A	17.95	17.64	B_1	7	8.0
B	4.0	6.60	B_2	7	-
C	13.0	13.20			

3. SIMULATED & MEASURED RESULT

The design and simulation of the two antennas has been carried out using the CST Microwave Studio. Experimental validation of the two designs was done by fabricating the two prototypes with optimized dimension and measuring the frequency response on a Rohde & Schwarz Vector Network Analyzer (ZVA-40). The fabricated antennas are shown in Fig. 4.

Fig 4: Photograph of Fabricated view of Antenna 1 & 2

The comparison of measured and simulated reflection coefficients are shown in Fig. 5 and Fig. 6. The Antenna 1 has a measured impedance bandwidth of around 8 GHz from 2.6 GHz to 10.6 GHz. The Antenna 2 has a measured impedance bandwidth of 7.7 GHz from 3 GHz to 10.7 GHz. The measured and simulated results are in good agreement except for some frequencies. The difference between the measured results and the simulated results is due to the fabrication tolerances, connection mis-alignment and uncertainty in the substrate thickness and the impedance response of the Sub-Miniature Version `A' (SMA) connectors used. Fig.7 shows a comparison of the simulated reflection coefficient of the two antennas. It can be seen from Fig. 7 that due to variation in the slot shape, antennas have different reflection loss values at same frequencies. In the Fig. it can be seen that Antenna 1 has smaller bandwidth. Its lower band starts from 2.54 GHz and it goes up to 9.626 GHz corresponding to an impedance bandwidth of 7.086 GHz. Response at higher end deteriorates because of improper matching between patch and slot. In Antenna 2, because of the change in slot shape, extra resonance is generated at higher frequency that causes expansion in impedance bandwidth.

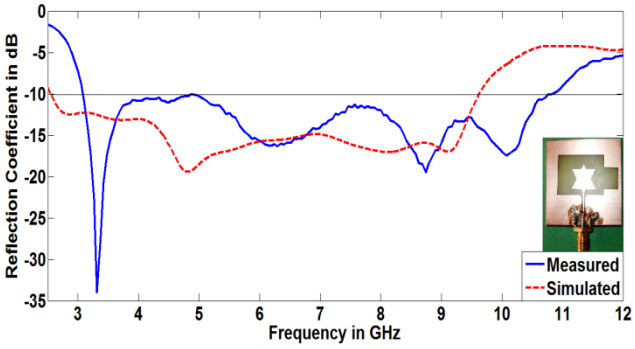

Fig 5: Measured & Simulated Reflection Coefficient of Antenna 1

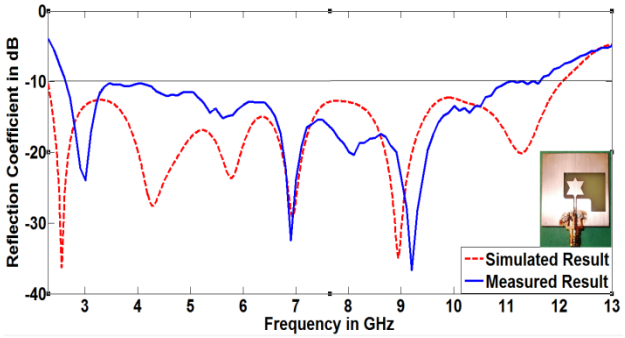

Fig 6: Measured & Simulated Reflection Coefficient of Antenna 2

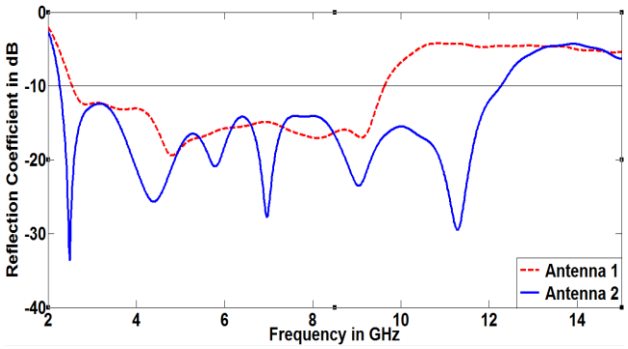

Fig 7: Simulated Reflection Coefficient of Antenna 1 and Antenna 2

3.1 Theoretical Discussions

The surface current distribution at different resonance frequencies are shown in Fig. 8. The red color shows the maximum current density while the blue shows the minimum current density. The surface current at 2.5 GHz shows two maxima along the slot, therefore it can be concluded that the resonance at 2.5 GHz is due to slot in the ground plane. The current distribution at 4.4 GHz shows increased current in the star shape patch, so the resonance at 4.4 GHz is due to the star shaped patch. The current density at 5.7 GHz shows four maxima along the slot therefore, the resonance at 5.7 is due to first harmonics of lowest resonance at 2.5 GHz.

By considering the current distribution, the first resonance can be approximated as

$$f_1 = \frac{c}{SL\sqrt{\varepsilon_{eff}}} \quad (1)$$

Here f_1 is the lowest resonance frequency in Hz, SL is the slot length in meter, c is the speed of light in m/sec and ε_{eff} is the effective relative permittivity. The second resonance frequency can be approximated by considering the height of the patch to λ/4 and it is given by

$$f_2 = \frac{c}{4L\sqrt{\varepsilon_{eff}}} \quad (2)$$

Here, L is the height of the star shaped patch. The first and second resonance frequencies are calculated and compared with simulated values as given in table 3. The difference between the calculated and simulated value of resonance frequency is due to the error involved in calculating the value of ε_{eff}.

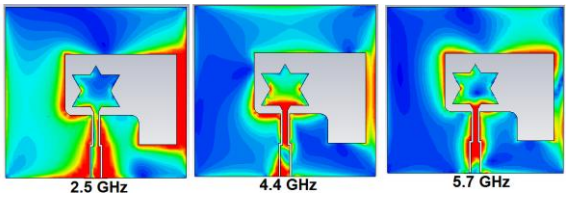

Fig 8: Current Distribution for Antenna 2 at Resonance Frequencies

Table 3. Calculated and Simulated Value of Resonance Frequency (in GHz)

Antenna	Calculated f_1	Simulated f_1	Calculated f_2	Simulated f_2
1	2.37	2.75	3.69	3.70
2	2.15	2.49	4.28	4.40

4. RADIATION PATTERNS, GAIN & EFFICIENCY

The radiation patterns of Antenna 2 are measured in an in-house anechoic chamber using antenna measurement system. A double ridged horn antenna is used as reference antenna. Figure 9 shows a comparison of measured and simulated radiation patterns at different frequencies. The simulated radiation patterns in both the plane are in good agreement with the measured radiation patterns. The nature of radiation patterns is Omni-directional in H-plane and bidirectional in E – plane. It is observed as the frequency increases, the nature of radiation patterns slightly changes which may be because of generation of cross polarization.

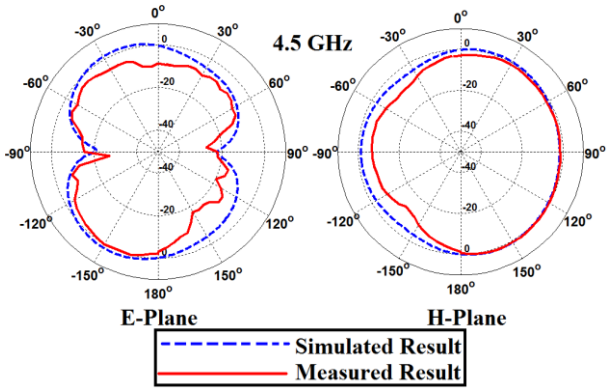

(a)

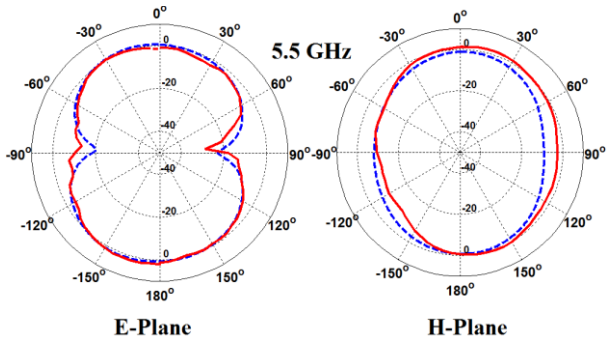

(b)

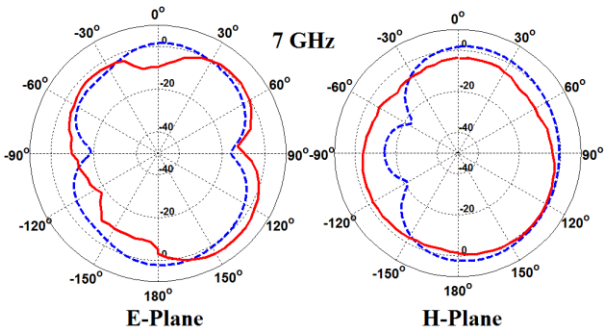

(c)

Fig 9: Radiation patterns of Antennas 2 at frequencies (a) 4.5 GHz (b) 5.5 GHz & (c) 7 GHz

The peak gain of both the antenna is simulated using CST MW studio software and shown in Figure 10. The peak gain increases at centre frequency as there is proper coupling of energy from patch to the slot as also seen from the return loss characteristics. Beyond a certain higher frequency, it starts decreasing because of mismatch of impedance as well as at higher frequency, dielectric losses and cross polarization increases. The radiation efficiency of the antenna was also simulated using CST MW Studio and is shown in Figure 11. The radiation efficiency of the antenna decreases as frequency increases. It comes down from 93% at 3 GHz to 80 % at 10.5 GHz. It is because dielectric loss of the FR4 substrate increases with frequency. The dip in radiation efficiency around 10.6 GHz in Antenna 1 is due to reflection coefficient just touching the - 10 dB.

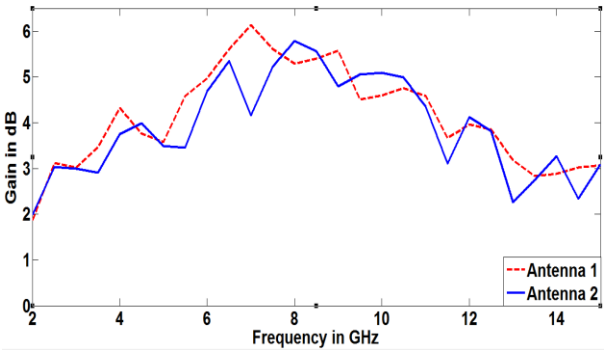

Fig 10: Simulated Peak gain of Antenna 1 and 2

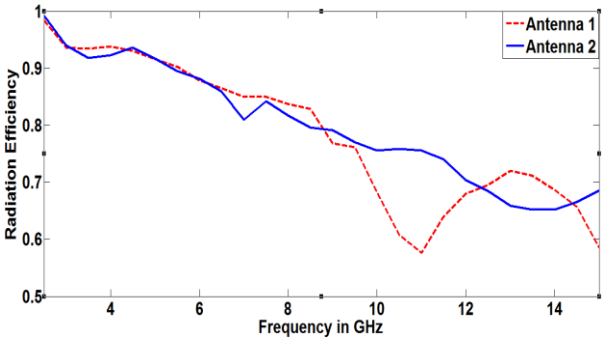

Fig 11: Simulated radiation Efficiency of Antenna 1 and 2

Figure 12 and 13 show the comparison between measured and simulated peak gain of the two antennas. The measured and simulated gain values are in good agreement with each other with a nearly constant gain values. Some deviation in measured gain can be because of alignment error in measurement.

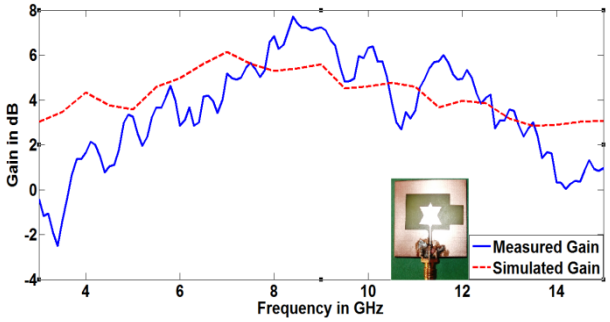

Fig 12: Measured & Simulated Peak gain of Antenna1

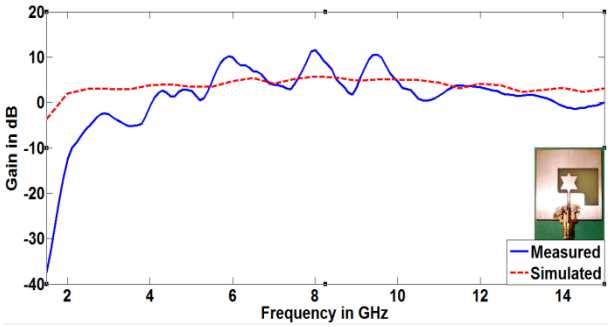

Fig 13: Measured & Simulated Peak gain of Antenna2

5. PARAMETRIC STUDY

The proposed slot antenna has been simulated for the various design parameters to achieve the UWB impedance bandwidth. The most effective design parameters are the gap between ground plane and patch, gap between feed and ground, ground width and ground length. These effective parameters have predicted by current distribution region of the antenna. All these critical design parameters are optimized in steps.

5.1 Effect of Variation of Patch Size

By changing the size of patch in Antenna 1, we are changing the position of second resonance. The second resonance frequency depends upon size of the patch, therefore changing the patch size causes change in second resonance frequency. For different patch dimensions the return loss curves are shown in Fig. 14. For higher values of patch size, interaction becomes poor and the return loss approaches the -10 dB line. The optimum value of patch dimensions is found to be 12 mm x12.392 mm. Fig 15 shows the effect of variation of the patch size on the return loss of Antenna 2. Because of diverse slot geometry and smaller patch size, a different optimized value of patch is chosen (10mm, 10.66mm). Here as well, change in second resonance can be seen because of change in patch size.

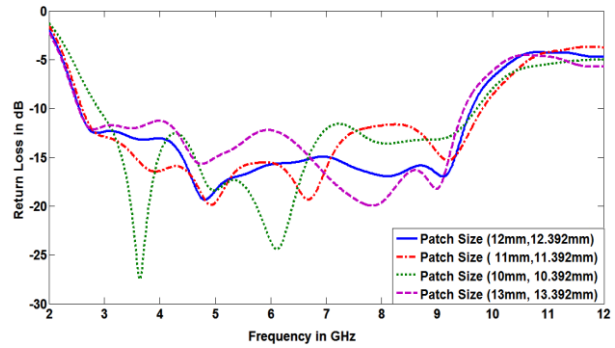

Fig 14: Study of variation of Patch size in Antenna 1

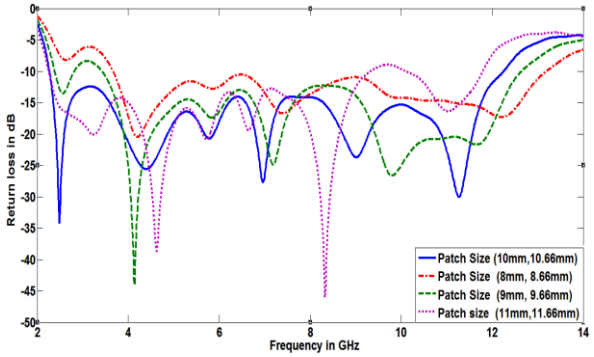

Fig 15: Study of variation of Patch size in Antenna 2

5.2 Effect of Variation of Feed Step Length

Fig.16 shows effect of variation of feed step length on the return loss of Antenna 2. The variation in feed step length affects the impedance matching of feed line. So by taking different combinations of upper and lower feed length, impedance matching is observed. For smaller values of upper feed length response improves in terms of bandwidth in lower as well as upper frequencies. But at in between frequencies response is closer to -10 dB line. Thus an optimized value of feed length combination is found where lower feed length is 6.60mm and upper feed length is 7.30 mm.

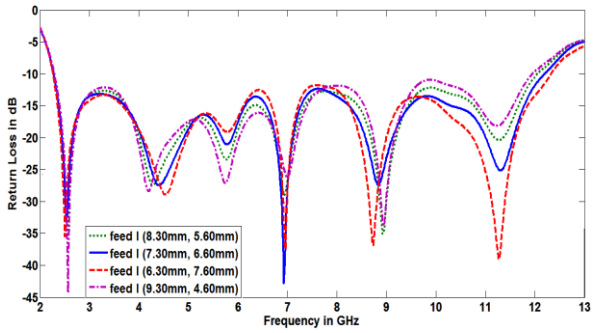

Fig 16: Study of variation of Feed length in Antenna 2

5.3 Effect of Variation of Feed Width

Feed width is an important factor as it is related to impedance matching between feed line and energy source. Here the gap is kept constant. The variation in feed width cause change in input impedance value of antenna, which in turn changes energy coupling from feed to patch. Fig. 17 shows effect of variation of feed width on return loss of antenna. For higher values of upper feed width, response improves in terms of bandwidth at upper frequencies but response approaches closer to -10dB line. An optimum value of feed width is upper feed width 1.018mm and lower feed width 1.93mm for best response. Here real part of impedance approaches closer to 50Ω and imaginary part approaches closer to zero.

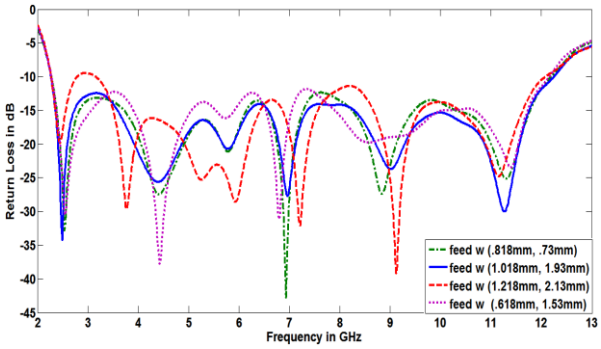

Fig 17: Study of variation of feed Width in Antenna 2

5.4 Effect of Variation of Feed Gap

Fig. 18 shows effect of variation of feed gap on return loss of Antenna 2. This is the gap between the feed line and the ground and tuning is essential to achieve proper impedance value of feed. As clear from Fig 6.4, for lower value of gap, improper impedance matching causes return loss to deteriorate. Thus by varying feed gap from 0.2 mm to 0.5 mm with a step size of 0.1mm and observing the return loss the optimum value of 0.3mm is obtained.

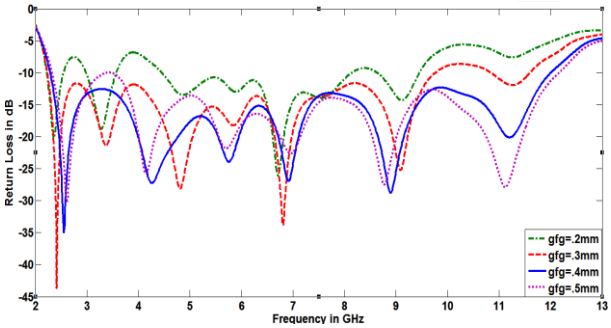

Fig 18: Study of variation of Feed gap in Antenna 2

5.5 Effect of Variation of Gap between Patch and Ground

Fig.19 shows effect of variation of separation between patch and ground on return loss of Antenna 2. This is the gap between the feed line and the patch that has to be optimized to maximize the coupling of energy between feed and patch. The variation in gap is affecting lower and higher end frequencies. If we take smaller value of gap return loss deteriorate at lower band of frequencies. And for larger gap, coupling becomes weaker and return loss approaches -10dB, thus an optimum value of gap is chose 0.7mm.

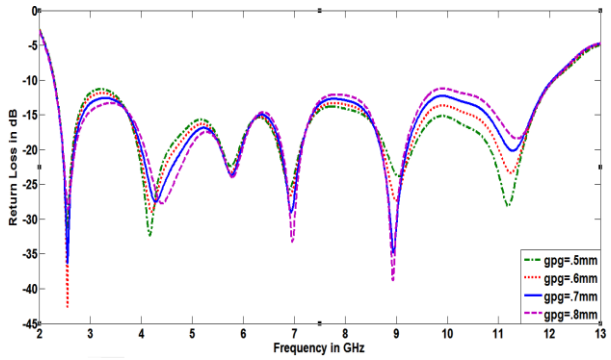

Fig 19: Study of variation of Patch gap in Antenna 2

6. CONCLUSIONS

A new rectangular CPW – feed slot antenna has been designed and validated experimentally. By employing a star shaped radiating patch with asymmetric slot, the measured impedance bandwidth starting from 2.836 GHz and extending well beyond the FCC UWB limit has been achieved (more 100% at the centre frequency of 7.25 GHz). The peak gain of the proposed antenna remains around 5 dB in the useful band. The proposed antenna can be used for UWB applications such as high speed data communications, medical imaging and vehicular radar.

7. ACKNOWLEDGEMENT

The first author acknowledges the financial support and facilities extended by the Defence Institute of Advanced Technology (Deemed University), Pune, India for carrying out the Research work.

8. REFRENCE

[1] G. R. Aiello and G. D. Rogerson, "Ultra-wideband Wireless Systems," Systems," IEEE Microwave Magazine, June, 2003, pp. 36-47.

[2] H. Schantz, The Art and Science of Ultra wideband Antennas, Artech House Inc., 2005.

[3] Narayan Prasad Agrawall, Girish Kumar, and K. P. Ray, "Wide-Band Planar Monopole Antennas", IEEE Transactions on Antennas and propagation , vol. 46, no. 2, February 1998, pp. 294-295,.

[4] M.A. Habib and T.A. Denidni, Design of a new wideband microstrip- fed circular slot antenna, Microwave Opt Technol Lett 48, (2006), 919–923.

[5] J. Liang, C.C.Chiau, X. Chen, and J. Yu, "Study of a circular disc monopole antenna for Ultra Wideband applications", 2004 International Symposium 00 Antennas and Propagation, pp. 8 1-84, Sendai, Japan, Aug. 2004, pp.17-21.

[6] Jianxin Liang, Lu Guo, Choo C. Chiau and Xiaodong Chen, "CPW-Fed Circular Disc Monopole Antenna for UWB Applications" IEEE AP-S 2005, pp.505-508.

[7] W.J. Lui, C.H. Cheng, and H.B. Zhu, Compact frequency notched ultra-wideband fractal printed slot antenna, IEEE Microwave Wireless Compon Lett 16 (2006), 224-226.

[8] M. Ding, R. Jin, J. Geng, and Q. Wu, Design of a CPW-fed ultrawideband fractal antenna, Microwave Opt Technol Lett 49 (2007), 173-176.

[9] Raj Kumar, Dhananjay Magar and K. K. Sawant,"On the design of inscribed triangle circular fractal antenna for UWB applications", Int. Journal of Electronics and Communication (AEU), Jan. 2012, pp. 68-75, Germany.

[10] Raj Kumar and K. K. Sawant, On the design of inscribed triangle non-concentric circular fractal antenna, Microwave and Optical Technology Letters, Vol.52, No. 12, Dec. 2010, 2696-2699.

[11] R.V.S. Rama Krishna and Raj Kumar "Design of ultra wideband trapezoidal shape slot antenna with circular polarization," AEU - International Journal of Electronics and Communications, Volume 67, Issue 12, pp. 1038–1047, December 2013,

[12] S. Barbarino and F. Consoli, "UWB circular slot antenna provided with an inverted-l notch filter for the 5 GHz WLAN band," Progress In Electromagnetic Research, Vol. 104, 1-13, 2010.